# Exploring the feasibility of optomechanical systems for temperature estimation in interferometric setups

Morteza Shirzad,[1,*] Rasoul Roknizadeh,[1,2,†] and Ali Mahdifar[1,2,‡]
[1]*Faculty of Physics, University of Isfahan, Isfahan 81764-73441, Iran*
[2]*Quantum Optics Group, University of Isfahan, Isfahan 81764-73441, Iran*

(Received 11 December 2023; accepted 11 April 2024; published 7 May 2024)

Accurate temperature measurement is critical in many scientific and engineering fields, so that researchers continuously strive to improve the accuracy, sensitivity, and robustness of the current measurement methods. In this paper, we propose a theoretical approach for temperature measurement using an optomechanical system in which the position of a mechanical oscillator is coupled to the cavity field. Our approach enables precise control and manipulation of both, resulting in highly accurate temperature measurements. We evaluate the accuracy of temperature estimation by using classical and quantum Fisher information, considering both open and closed systems, and investigate entanglement effects of the primary field mode. Our findings indicate that increasing entanglement at the input made reduces measurement time and increases sensitivity in estimating the temperature. However, we observe that quantum coherence is destroyed by decoherence, leading to reduced performance of quantum systems. Furthermore, we show that the Fisher information of the system is robust against mechanical decoherence, but significantly damped due to optical decoherence. We discuss the limitations and challenges of our method and suggest possible applications and future directions for our research. Finally, we determine the accuracy of temperature estimation for a typical optomechanical system based on phase values measured in the closed system. Our results demonstrate the potential of optomechanical systems for highly accurate temperature measurement and their robustness against decoherence. This study can provide insights into the field of temperature measurement, offering a theoretical approach that can be applied in many scientific and engineering applications.

DOI: 10.1103/PhysRevA.109.053509

## I. INTRODUCTION

In recent decades quantum technology has made significant advancements in cryptography, metrology, and computing [1–5]. However, accurate temperature measurement is critical for the successful application of these quantum devices. To achieve precise temperature estimation at the quantum scale, researchers are exploring a unique approach [6–13]. The concept of temperature primarily refers to macroscopic phenomena and does not have a direct connection to the quantum realm. This presents a significant obstacle when attempting to estimate temperature estimation in quantum content. Moreover, the exponential nature of temperature within the functions that characterize the system's density operator adds further complicated complexity to the situation. Instead, researchers are using estimation theory to measure other physical quantities, such as average kinetic energy, to determine temperature indirectly [14]. Accurate temperature assessment holds immense potential for unlocking the full potential of quantum technologies and paving the way for further advancements in the field.

The field of quantum metrology explores the fundamental limits of estimation error using the quantum Cramér-Rao bound (QCRB) [15–20]. Through the utilization of quantum resources such as entanglement and quantum correlations, researchers can achieve measurement precision beyond classical limits. By increasing the number of probes or measurements, one can approach the coveted "Heisenberg limit" of $1/N$, where $N$ represents the number of inquiries [21–29].

To improve the accuracy of the measurements, it is possible to employ quantum resources, such as entanglement. To this end, the entangled NOON states can be employed to deal with an entangled probe. The NOON states which are of great importance in theoretical studies, have successfully generated (up to $N = 9$ phonons) in a single trapped ion using a deterministic method [30]. This method is applicable to various photonic or phononic systems, and enables generation and verification of high NOON states. Another efficient technique was proposed to generate photonic NOON states using the rapid population passage technique via the shortcut to adiabaticity. The feasibility of this proposal is demonstrated with experimental circuit QED systems [31].

The potential for accurate and simultaneous measurement of various parameters in a nonlinear medium without quantum limitations was investigated by maximizing the quantum Fisher information function for the coherent and squeezed input state parameters [32]. However, the study of natural quantum systems involves understanding their interactions with the environment, as this interaction can significantly impact the accuracy and reliability of quantum measurements. Therefore, thorough research and analysis are necessary to

*m.shirzad@sci.ui.ac.ir
†rokni@sci.ui.ac.ir
‡a.mahdifar@sci.ui.ac.ir

 

gain a comprehensive understanding of quantum systems' behavior in different environmental conditions. A recent study focused on jointly estimating loss and nonlinearity in driven-dissipative Kerr resonators [33]. They found that, for the pure state, the resonators are asymptotically classical and is possible to estimate two parameters without additional quantum noise. Additionally, the study identified optimal interaction time and driving amplitude to improve the ultimate precision of the estimates.

The present article primarily focuses on the optomechanical system's precision in measuring temperature. Nonetheless, it also addresses critical inquiries about temperature measurement methodologies and intricacies in the references, for instance, using an optomechanical system as a primary thermometer involves an indirect measurement of the phonon number of the mechanical oscillator, which is directly proportional to the system's energy [34]. In a secondary thermometry method, the temperature is estimated by measuring the relative phase obtained from a known reference temperature sample and an unknown temperature sample [7,35]. This article describes a different approach that surpasses the Cramér-Rao limit and enhances precision using quantum resources. This approach has been extensively researched in parameter estimation. Recent studies focused on defining and quantifying quantum correlations in composite states. These studies explored the operational relevance of quantum technology and probe the classical-quantum correlation boundary. The investigation provides valuable insights into the underlying mechanisms of optomechanical systems and their practical applications [36–39].

This paper is organized as follows. In Sec. II A, we provide an overview of quantum parameter estimation and introduce the Cramér-Rao bound (CRB), which sets a fundamental limit on the accuracy of any unbiased estimator. We also define the Fisher information (FI) based on the conditional probability of measuring desirable observables. Then, in Sec. II B we describe the optomechanical system in the Michelson interferometer. In Sec. III A, we measure the phase parameter in the measurement output to obtain the FI of the closed system. Next, we examine the system as an open system to explore the effects of loss in the field and mechanical subsystem. This section aims to provide a comprehensive understanding of how to monitor these systems and obtain accurate information. To delve into the quantum Fisher information (QFI), we utilize the symmetric logarithmic operator in Sec. III B to optimize the FI across all possible measurements with positive operator-valued measurement (POVM). Moving on to the third and final Sec. III C, we assess the accuracy of temperature measurement in a closed system based on phase outputs. Finally, in Sec. IV, we provide our conclusions.

## II. PARAMETER ESTIMATION AND SYSTEM SPECIFICATION

In quantum physics, four fundamental steps must be followed when performing measurements. The initial and foremost step entails closely monitoring the quantum sensor and ensuring that its initial state is appropriately prepared. Subsequently, it is imperative to interact with the desired signal robustly while simultaneously mitigating any potential interference. Once this has been accomplished, it is crucial to read the final state and determine the density of the sensor. The ultimate step involves using phase and parameter estimation techniques to ascertain the precise magnitude of the signal.

### A. Parameter estimation and the Cramér-Rao limit

The problem of parameter estimation lies in identifying a continuous or discrete parameter, denoted by $\theta$, which is a result of the interaction between two or more subsystems and encoded in the system's state $\rho_\theta$. The process of parameter estimation is typically broken down into three distinct steps, namely, (i) the interaction between a state with known parameters, referred to as the quantum probe, and a state whose parameters are unknown, i.e., the quantum object; (ii) the configuration setup involving a detector that measures the state of the quantum probe; and (iii) the utilization of data analysis techniques to determine the desired parameter value. The accuracy of the estimated parameter can be evaluated by using the renowned Cramér-Rao bound (CRB). It is pertinent to note that the effectiveness of this protocol can be enhanced by carefully selecting appropriate features and quantum resources to increase the sensitivity of the estimation process.

Following the interaction and measurement, the state of the quantum probe undergoes analysis via the POVM, denoted as $\mathcal{M}^{\{\mathrm{POVM}\}} = \{\hat{E}_x^{(N)}\}$ [40]. This process is repeated on $N$ identical independent copies of the quantum probe, resulting in measurements that pertain to the set $x$. The probability of each element of this set occurring is given by $\mathcal{P}(x|\theta) = \mathrm{Tr}\{\hat{E}_x^{(N)}\,\rho_\theta^{\otimes N}\}$ [40]. We utilize standard data processing methods and identify its correlation with the estimated parameters to determine the value of the unknown parameter.

The CRB stands as a vital constraint on the level of precision that can be achieved in parameter estimation and serves as a standard against which the performance of any estimator can be evaluated. It is worth noting that the CRB relies on the underlying statistical model of the data and the specific estimator utilized and may only be attainable under certain circumstances. Under the assumption of asymptotically unbiased parameter estimation, the CRB offers a means of expressing the variance of the estimated parameter ($\Delta\theta$) as a function of the FI matrix [18,40,41]

$$\Delta\theta \geqslant 1/N\sqrt{\mathcal{F}(\rho_\theta)}. \tag{1}$$

FI is the amount of information that a given random variable contains regarding the parameter of interest. The concept of FI can be precisely defined in terms of of CRB as

$$\mathcal{F}(\rho_\theta) \equiv \sum_x \mathcal{P}^{-1}(x|\theta)\,[\partial_\theta \mathcal{P}(x|\theta)]^2. \tag{2}$$

The achievement of a particular sensitivity level through a measurement protocol can be evaluated using the classical Fisher function and CRB. These customary functions do not require the maximization of the Fisher function for all sets of $\mathcal{M}^{\{\mathrm{POVM}\}}$, which are known as the classical boundary. The matrix capacity of the protocol to achieve the optimal sensitivity as predicted by theory can be investigated while taking into account the experiment's limitations [20,24,42].

We can identify where FI reaches its most significant potential by studying the CR inequality. To achieve optimal

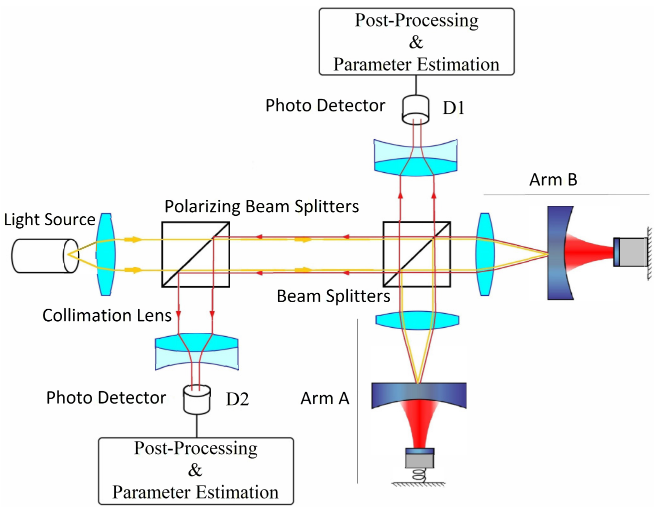


FIG. 1. Schematic representation of the proposed experimental setup utilizing a Michelson interferometer for a single photon. The $A$ and $B$ arms are equipped with high-precision slots and a cavity with a tiny end mirror mounted on a micromechanical oscillator in the $A$ arm. Two single-photon detectors, $D1$ and $D2$, monitor the photons that leak out of each of the slits [44,45].

sensitivity, examining all feasible combinations of POVM operators is necessary to determine when Eq. (1) yields an equality, rather than an inequality relation. This approach produces outcomes referred to as 'quantum Fisher information" (QFI) and "quantum Cramér-Rao bound" (QCRB), which can be utilized to establish the maximum level of measurement accuracy, even in the absence of quantum resources [18,19].

In statistical mechanics, the optimal estimation of the temperature parameter for a given system can be attained through an analysis of the measurement statistics of the energy operator. However, when energy measurement becomes increasingly intricate, the temperature value can be estimated by investigating temperature-dependent quantities. It can be demonstrated that, in the evaluation of the temperature parameter, the measurement of the energy-dependent function of the system satisfies the inequality saturation condition and yields the QCRB ($B$) [43].

The present study employs the symmetric logarithmic derivative (SLD) operator, as proposed in the Fisher function optimization approach, to achieve its research objective. For temperature, the operator is defined as [7]

$$\hat{\Lambda}_T = \frac{1}{k_B T^2}(\hat{H} - \langle \hat{H} \rangle). \tag{3}$$

Therefore, the uncertainty obtained from the QCRB will be as follows:

$$\sqrt{N}\Delta T \geqslant \frac{1}{\sqrt{\mathcal{F}(T)}} = \frac{k_B T^2}{\Delta \hat{H}}. \tag{4}$$

### B. Characterization of the optomechanical system

Here, we elaborate on the application of the optomechanical system, which consists of a cavity and a movable mirror, within the framework of the Michelson interferometer. As shown in Fig. 1, one arm of the interferometer incorporates a high-finesse optomechanical cavity, while the other arm features an optical cavity, showcasing the versatility of this configuration in various practical scenarios. This particular configuration has proven invaluable in observing the impact of a single photon on a macroscopic mechanical component [44], as well as the exploration of the nonlinear effects of the system [46].

Furthermore, it enables the analysis of the interaction between the field and mechanical modes, thus providing insight into the intricate dynamics of the system [45]. The setup involves a polarizing beam splitter situated at the input of the structure that ensures an equal likelihood of photon entrance into each interferometer's arms. The mechanical component achieves equilibrium with a thermal reservoir maintained at a particular temperature, denoted as $T$. The radiation pressure of light influences the oscillatory motion of this mechanical component, resulting in a nonlinear interaction that yields a correlation between the mechanical and optical subsystems. In addition, a pair of single-photon detectors are situated at the two outputs of the interferometer to detect the single photons produced. The interferometry process is conducted by measuring the phase difference between the outputs.

We employ the nonlinear variant of the optomechanical system as follows [34,47,48]:

$$\hat{H}_{\mathrm{OM}} = \hbar\,\omega_{\mathrm{C}}\,\hat{a}^\dagger\hat{a} + \hbar\,\omega_{\mathrm{M}}\,\hat{b}^\dagger\hat{b} - g_0\,\hat{a}^\dagger\hat{a}(\hat{b}^\dagger + \hat{b}). \tag{5}$$

This system operates using two distinct types of operators: $\hat{a}(\hat{a}^\dagger)$ and $\hat{b}(\hat{b}^\dagger)$. These operators serve the purpose of annihilation and creation of optical and mechanical modes, respectively. We denote the frequency of the cavity and the mechanical oscillator by $\omega_{\mathrm{C}}$ and $\omega_{\mathrm{M}}$. Meanwhile, $g_0$ is representative of the optomechanical coupling.

The initial density operator of the optomechanical system can be expressed as the tensor product of the density operators of the mechanical and field modes

$$\hat{\rho}_{\mathrm{OM}}(0) = \hat{\rho}_{\mathrm{M}}(0) \otimes \hat{\rho}_{\mathrm{O}}(0). \tag{6}$$

The initial assumption is that the mechanical oscillator is in equilibrium with its surrounding environment at a given temperature, denoted as $T$. Consequently, we can effectively describe the probability distribution of the mechanical mode through the utilization of the Gibbs state, which represents the density operator as follows:

$$\hat{\rho}_{\mathrm{M}}(0) = \sum_j \rho_{j\,j}\,|j\rangle\langle j|. \tag{7}$$

Here $\rho_{j\,j} = n_{\mathrm{th}}^j/(1+n_{\mathrm{th}})^{j+1}$, $n_{\mathrm{th}} = (e^{\beta\hbar\,\omega_{\mathrm{M}}} - 1)^{-1}$, and $\beta = 1/k_B T$.

Utilizing entangled photon modes is a promising approach to enhance accuracy and sensitivity in the field of quantum measurement and parameter estimation. Here, we use the NOON quantum state

$$|\mathrm{NOON}\rangle = (|n_{\mathrm{A}}, 0_{\mathrm{B}}\rangle + |0_{\mathrm{A}}, n_{\mathrm{B}}\rangle)/\sqrt{2}, \tag{8}$$

for the interferometric system with $N$ injected photons. Here, the state $|n_{\mathrm{A}}, m_{\mathrm{B}}\rangle$ describes the mode that contains $n(m)$ photons in arm $A(B)$. We multiply the field mode state with the Gibbs state of the mechanical mode using tensor multiplication to establish the optomechanical system's initial state.

By initializing the optomechanical system with an entangled NOON state in the interferometer input, we can achieve the initial state of the optomechanical system as follows:

$$\begin{aligned}\hat{\rho}_{\mathrm{OM}}(0) &= \hat{\rho}_{\mathrm{M}}(0)\otimes\hat{\rho}_{\mathrm{O}}(0)\\ &= \frac{1}{2}\sum_{j=0}^{\infty}\rho_{jj}|j\rangle\langle j|\\ &\quad\otimes(|0_{\mathrm{A}}\,n_{\mathrm{B}}\rangle\langle n_{\mathrm{B}}\,0_{\mathrm{A}}| + |0_{\mathrm{A}}\,n_{\mathrm{B}}\rangle\langle 0_{\mathrm{B}}\,n_{\mathrm{A}}|\\ &\quad + |n_{\mathrm{A}}\,0_{\mathrm{B}}\rangle\langle n_{\mathrm{B}}\,0_{\mathrm{A}}| + |n_{\mathrm{A}}\,0_{\mathrm{B}}\rangle\langle 0_{\mathrm{B}}\,n_{\mathrm{A}}|).\end{aligned} \tag{9}$$

## III. ACCURACY OF TEMPERATURE ESTIMATION WITH OPTOMECHANICAL SYSTEM

We first measure the classical FI from the phase output of the system to estimate the temperature parameter. Based on this, we derive the classical CRB and analyze the system in three distinct cases: closed system, open system with mechanical loss, and open system with optical loss. Next, we evaluate the system based on energy measurement and determine the QFI to estimate the temperature evaluation. We then specify the QCRB and analyze the system in the same three distinct situation. Lastly, we determine the sensitivity of temperature parameter estimation, as a dependent variable for phase by measuring the phase in the system output. Overall, this analysis provides a comprehensive understanding of the system under examination and the various factors that impact its performance in different states.

### A. FI behavior based on phase operator measurement

To determine FI upon the phase measurement, the initial approach involves utilizing the conditional probability function, derived from the projection measurement of the phase operator and subsequently extracting the classical FI. However, it is noteworthy that measuring the precise magnitude of the partial phase difference, which serves as the central objective of interferometry and can be utilized to determine various physical properties of systems, presents a significant challenge. This task necessitates a well-defined phase operator, and for this purpose, we opted for the non-Hermitian Suskind-Galgower phase operator

$$\sin\hat{\phi} = \sum_{n=0}^{\infty}(|n\rangle\langle n+1| + |n+1\rangle\langle n|). \tag{10}$$

This particular operator possesses eigenstates with distinct phases, and by exploitation of its self-adjointness property, we can derive a well-defined Hermitian operator [50].

In the context of the NOON mode, wherein the photon number is restricted to only two values, namely, zero and $n$, the most suitable projection measurement operator which can be utilized to extract the overall phase shift in the interferometer is [40,51–53]

$$\hat{\phi}^{\{n\}} = |n_{\mathrm{A}},\,0_{\mathrm{B}}\rangle\langle n_{\mathrm{B}},\,0_{\mathrm{A}}| + |0_{\mathrm{A}},\,n_{\mathrm{B}}\rangle\langle 0_{\mathrm{B}},\,n_{\mathrm{A}}|. \tag{11}$$

The evaluation of the system's state is accomplished by the output of the interferometer utilizing the phase projection operator following the time transformation. Subsequently, through an analysis of the impact of the phase operator on the system state, it becomes feasible to compute the probability function $\mathcal{P}(\phi|T) = \mathrm{Tr}\{\hat{\phi}\,\rho_{\mathrm{OM}}(\tau)\}$, which, in turn, facilitates the determination of the FI function [40,51,52,54]. This procedure yields the following outcome for a closed system:

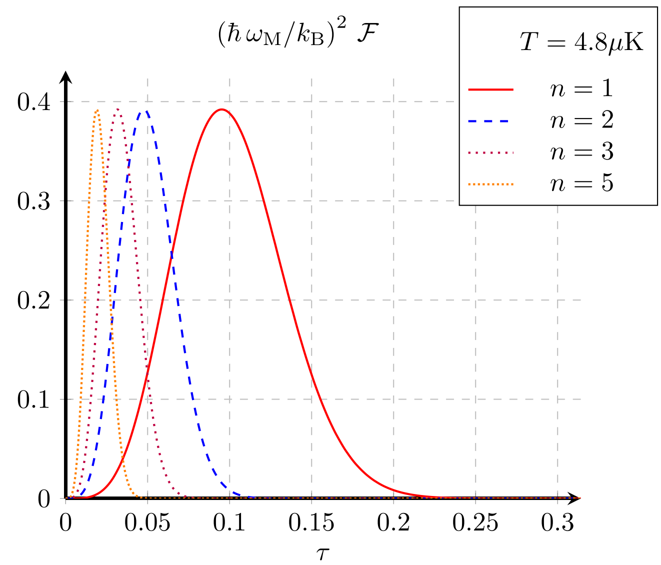


FIG. 2. Changes in Fischer information related to an optomechanical cavity of a closed system versus dimensionless time for different numbers of photons. This diagram is drawn based on experimental data for optomechanical cavities that satisfy the condition $g_0 \gg \omega_{\mathrm{M}}$, The related parameters are $g_{\mathrm{M}} = g_0/\omega_{\mathrm{M}} = 14.29$, $\gamma_{\mathrm{M}} = \gamma/\omega_{\mathrm{M}} = 0.024$, $T = 4.8\,\mu$K, and $\kappa_{\mathrm{M}} = \kappa/\omega_{\mathrm{M}} = 15.7$ [49].

$$\begin{aligned}\bar{\mathcal{F}}^{\hat{\phi}}_{\mathrm{NOON}} &= \tfrac{1}{16}\,n^4\,|\eta(\tau)|^4\,\cos[n^2\,\theta_{\mathrm{s}}(\tau)]\\ &\quad\times x^4\,\mathrm{csch}^4\!\left(\tfrac{1}{2}x\right)e^{-\frac{1}{2}n^2\,|\eta(\tau)|^2\,\coth(\frac{x}{2})},\end{aligned} \tag{12}$$

where in $\bar{\mathcal{F}} = (\hbar\,\omega_{\mathrm{M}}/k_{\mathrm{B}})^2\,\mathcal{F}$, $\theta_{\mathrm{s}}(\tau) = \tau - \sin(\tau)$, $|\eta(\tau)|^2 = 4\,g_{\mathrm{M}}^2\,\sin^2(\tau/2)$, $g_{\mathrm{M}} = g_0/\omega_{\mathrm{M}}$, $x = \beta\hbar\,\omega_{\mathrm{M}}$, $\tau = \omega_{\mathrm{M}}\,t$, and $\beta = k_{\mathrm{B}}\,T$. When analyzing the variations in Fisher information using the ratio of the coupling coefficient to the mechanical frequency multiplied by the number of photons [$\alpha = n^2\,g_{\mathrm{M}}^2\,(\tau/2)^2\,\coth(x/2)$], we find that the result is a consistently increasing function like $\alpha^2\,e^{-2\alpha}$. However, for this function to give a suitable value for small values of $\tau$, either the number of entangled photons ($n$) must be very high or the $g_{\mathrm{M}}$ coefficient must surpass a value of significantly larger than 1.

Figure 2 displays the changes in FI of the system as the number of distinct photons varies. Increasing the number of entangled photons results in achieving maximum FI in a shorter time, allowing for higher rates of simultaneous measurements. It is important to note that to obtain this phenomenon, the optomechanical coupling coefficient should be significantly larger than the frequency of the mechanical mode ($g_0 \gg \omega_{\mathrm{M}}$).

The oscillating part $\cos[n^2\,\theta_{\mathrm{s}}(\tau)]$ is the primary factor responsible for the oscillating nature of the FI, resulting in alternating periods of fall and rise in the absence of any losses within the system when the dimensionless time scale $\tau$ is in the significant range, as shown in Eq. (12) and Fig. 2. However, it is crucial to note that the practical application of the timescale requires the fulfillment of the condition $\tau \ll 1$. The maximum FI in this limit is achieved at $\tau = 2\sqrt{\tanh(x/2)}/n\,g_{\rm M}$, equivalent to $\bar{\mathcal{F}} = 4\,e^{-2}\,x^4\,{\rm csch}^2(x)$. By substituting the maximum FI value into the CRB, we can determine the standard deviation for temperature estimation as

$$\frac{\Delta T}{T} \leqslant \frac{1}{N}\,\frac{e\,\sinh(x)}{2\,x}, \tag{13}$$

where the constant $e$ is the Euler's number. The determination of the number of measurements, denoted by $N$, is contingent upon the available total measurement time $\tau$ and the additional time required for initialization, manipulation, and reading the results [40]. Consequently, the precision of the temperature measurement at a specific temperature can be enhanced by decreasing the ratio of classical energy $k_{\rm B}\,T$ to quantum energy $\hbar\,\omega_{\rm M}$, which aligns with the fundamental principles of quantum mechanics.

The data depicted in the Fig. 2 presented herein reveal that, under the condition $\tau \ll 1$, the NOON mode outperforms the single-photon mode in terms of FI, yielding an increase in FI proportional to $n^4$. Notably, entangling $n$ photons leads to a reduction in the time frame required to achieve maximum FI by a factor of $1/n$. These observations have considerable implications, as increasing the number of entangled photons enhances the number of repetitions within a given time frame, thus improving measurement precision. Notably, the application of the NOON state is instrumental in achieving the Heisenberg limit for successive measurements with a predetermined time interval. These findings underscore the potential of entanglement-based techniques in realizing highly accurate measurements and highlight the importance of considering the NOON state when selecting the appropriate measurement approach.

To understand how the environment impacts the optomechanical system, we use the Lindblad master equation to model the evolution of the system's state over time. The Lindblad formulation enables us to rigorously explore all the loss mechanisms and noise sources present in the system's surroundings. This allows for a comprehensive investigation into how these environmental factors shape the behavior and capabilities of the optomechanical system. Specifically, we consider the system under two scenarios: first, we only consider mechanical loss, and then we investigate optical loss (see Appendixes B and C for more details). The FI for the open system with mechanical loss is given by

$$\bar{\mathcal{F}}^{\gamma,\hat{\phi}}_{\textsf{NOON}} = \tfrac{1}{16}\,[n^2\,|\beta_n(\tau)|^2 + 2\,\theta_\gamma(\tau)]^2\,\cos[n^2\,\theta_{\rm t}(\tau)] \times x^4\,{\rm csch}^4\!\left(\tfrac{1}{2}x\right)e^{-\frac{1}{2}\,[n^2\,|\beta_n(\tau)|^2+2\,\theta_\gamma(\tau)]^2\,\coth(\frac{x}{2})}, \tag{14}$$

where $\gamma$ is mechanical loss coefficient, $\gamma_{\rm M} = \gamma/\omega_{\rm M}$, and

$$\theta_{\rm t}(\tau) = \tfrac{e^{-\gamma_{\rm M}\,\tau/2}}{(\gamma_{\rm M}^2+4)}\left[e^{\gamma_{\rm M}\,\tau/2}\left(\gamma_{\rm M}^2\,\tau - 4\,\gamma_{\rm M} + 4\,\tau\right) + 4\,\gamma_{\rm M}\,\cos(\tau) + \left(\gamma_{\rm M}^2 - 4\right)\sin(\tau)\right],$$

$$\theta_{\gamma_{\rm M}}(\tau) = \tfrac{2\,\gamma_{\rm M}\,\tau}{(\gamma_{\rm M}^2+4)}\left\{\left(\gamma_{\rm M}^2 + 4\right)\tau - 4\,\gamma_{\rm M} + 4[\gamma_{\rm M}\,\cos(\tau) - 2\,\sin(\tau)]e^{-\gamma_{\rm M}\,\tau/2}\right\},$$

$$\beta_n(\tau) = \tfrac{2\,i\,g_{\rm M}\,n}{\gamma_{\rm M}+2\,i}\,[1 - e^{-(\gamma_{\rm M}+2\,i)\tau/2}].$$

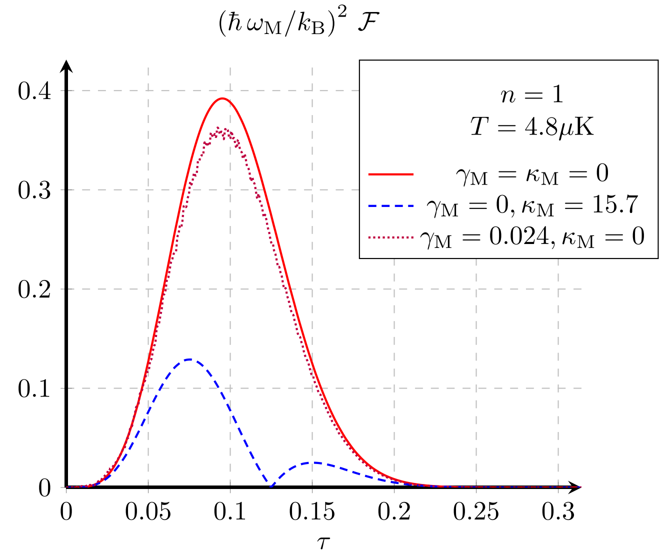


FIG. 3. FI in closed and open optomechanical systems with varying loss mechanisms, versus dimensionless time $\tau$. The data are based on experimental measurements of optomechanical cavities with $g_0 \gg \omega_{\rm M}$, where $g_{\rm M} = 14.29$, $\gamma_{\rm M} = 0.024$, and $\kappa_{\rm M} = 15.7$ [49].

Equation (14) highlights that mechanical loss results in amplitude modulation FI. Also, in the scenario where optical loss is present, FI is obtained as

$$\bar{\mathcal{F}}^{\kappa,\hat{\phi}}_{\textsf{NOON}} = \tfrac{1}{16}\left(1 - \tfrac{1}{2}\,n\,\kappa_{\rm M}\,\tau\right)|\eta(\tau)|^4\,\cos[n^2\,\theta_{\rm s}(\tau)] \times n^4\,x^4\,{\rm csch}^4\!\left(\tfrac{1}{2}x\right)e^{-\frac{1}{2}\,n^2\,|\eta(\tau)|^2\,\coth(\frac{x}{2})}, \tag{15}$$

where $\kappa_{\rm M} = \kappa/\omega_{\rm M}$, $\kappa$ is optical loss coefficient and $\theta_{\rm s}(\tau) = \tau - \sin(\tau)$. The presence of optical loss leads to strong damping of the FI function, as is clear by the term $(1 - \frac{1}{2}\,n\,\kappa_{\rm M}\,\tau)$.

To gain better insight into the effect of loss, we plot these FI's versus dimensionless time $\tau = \omega_{\rm M}\,t$ in Fig. 3. The figure clearly shows a significant decrease in the FI with increasing optical loss in the open system, while the effect of mechanical loss is minimal. Equation (15) indicates that optical loss is proportional to $1 - \kappa_{\rm M}\,\tau/2$, resulting in a linear decrease in FI. This representation primarily focuses on the interaction of a single photon with different coupling coefficients within the optomechanical cavity.

### B. FI behavior based on energy operator measurement

Within thermal systems, metrology serves two distinct purposes: the estimation of temperature, or thermometry, and the estimation of the coupling coefficient of field and mechanical modes in the Hamiltonian. Thermometry is a relatively straightforward process, yielding outcomes that are universal and not dependent on a specific model. If we consider a quantum system that is in thermal equilibrium with a heat source at a given temperature $T$, then the Gibbs model can be used to describe the density matrix of the system. Specifically, if the system's Hamiltonian is represented by $\hat{H}$, its thermal state can be defined as follows:

$$\rho^T = \mathcal{Z}^{-1}\,e^{-\hat{H}/k_{\rm B}\,T}, \tag{16}$$

where $\mathcal{Z} = \mathrm{Tr}\{e^{-\hat{H}/k_B T}\}$ is the partition function. The present discourse acknowledges the adiabatic nature of all the relevant parameters, ensuring that the Gibbs state consistently characterizes the system.

To measure temperature, one typically employs a thermometer that is considerably smaller than the medium being measured. This allows the thermometer to reach thermal equilibrium with the medium, effectively becoming isothermal; By doing so, the temperature of the sample can be deduced by reading the thermometer. We use this standard thermometry process to apply in the quantum state by obtaining the temperature of the sample through suitable measurement on the "steady state" of a thermometer that is isothermal with the environment. Through performing a large number of independent experiments, a reasonably accurate estimate of the temperature $T$ of the sample can be determined. However, to determine the minimum error associated with the estimation, QFI ($\mathcal{F}_T$) can be used in the QCRB inequality. Thus, one can consider QFI as determining the temperature sensitivity, which should have the most considerable possible value to maximize the accuracy in the estimation process.

To determine the QFI of a system, we use Eq. (4), which can provide the maximum FI per SLD operator. To do this, we need to calculate the expected values of the first order ($\langle \hat{H} \rangle$) and second order ($\langle \hat{H}^2 \rangle$) moments of the energy based on the Hamiltonian (5) (calculations are outlined in Appendix D).

Assuming the optomechanical system to be an isolated system that involves an ensemble consisting of particles associated with the field and mechanical modes, the quantum equivalent of this ensemble, i.e., the Gibbs density matrix of the system comprising the field and mechanical modes under the influence of the optomechanical interaction described by the $\hat{H}_{\mathrm{OM}}$ Hamiltonian, is derived as follows [55]:

$$\hat{\rho} = \sum_{j=0}^{\infty} |N;\, j, Ng_0/\omega_{\mathrm{M}}\rangle\langle Ng_0/\omega_{\mathrm{M}}, j;\, N|\, \frac{e^{-\beta \hat{H}_{\mathrm{OM}}}}{\mathcal{Z}}. \tag{17}$$

The QFI for a stationary system which necessitates the determination of the energy variance, is calculated as follows:

$$\bar{\mathcal{Q}}_G = \tfrac{1}{4}\, x^4 \mathrm{csch}^2(\tfrac{1}{2}\, x). \tag{18}$$

At $x = 3.83$, the QFI attains its maximum, with the value $\bar{\mathcal{Q}}_G = 4.88$. This result suggests that obtaining a sensitive measurement is achievable, regardless of the temperature, if the quantum to classical energy ratio is in proximity to the desired value.

Furthermore, as the variance is a limited quantity, it is feasible to compute the maximum energy variance and utilize it to analyze optomechanical energy behavior, determine optimal measurement conditions related to energy, and understand how the energy levels are arranged in the system [43]. We put $\partial_{E_N} \Delta \hat{H}_{\mathrm{O}}^2 = 0$, consequently, it can be deduced that either $j$ and $k$ are equal, or the following relationship holds:

$$\hbar\, \omega_{\mathrm{M}}(j + k) = 2(\langle \hat{H} \rangle + k_{\mathrm{B}}\, T - \hbar\, \omega_{\mathrm{M}} N\, \epsilon_N), \tag{19}$$

in which we have $\epsilon_N = (\omega_{\mathrm{R}}/\omega_{\mathrm{M}}) - (g_0^2/\omega_{\mathrm{M}}^2)N$ (see Appendix D for more information). This result implies that the optomechanical system in the bounded ensemble has induced the mechanical oscillator to exhibit characteristics of a two-level system.

The QFI of a Michelson interferometric setup, illustrated in Fig. 1, in a closed system and after a duration of time $t$, is computed as follows:

$$\bar{\mathcal{Q}}_{\mathrm{NOON}} = \tfrac{1}{4}\, x^4\, \mathrm{csch}^2(\tfrac{1}{2}\, x)\left[1 + n^2\, g_{\mathrm{M}}^2\, \sinh(x)\right]. \tag{20}$$

As evidenced by Eq. (20), the term within bracket is always larger than unity, and its value depends on factors such as the number of photons, physical characteristic of the mechanical state, and the hyperbolic pattern of the thermodynamic-to-quantum energy ratio. The optomechanical coupling between the field and mechanical states brings about this phenomenon. As a result, it can be concluded that the optomechanical coupling leads to an increase in the quantum Fischer information. The magnitude of this increase is directly proportional to three factors: the number of entangled photons in the field state ($n$), the ratio of the optomechanical coupling to the frequency of the mechanical oscillator ($g_{\mathrm{M}}$), and the argument of the hyperbolic function, which is the ratio of quantum to classical energy [$\sinh(x)$]. Equation (20) indicates that as the proportion of quantum energy to classical energy increases, the Fischer information attains its maximum value within a particular temperature interval.

In presence of mechanical loss, one can derive the QFI by calculating the variance in energy. To obtain this information, for a small loss coefficient, we have

$$\bar{\mathcal{Q}}^{\gamma}_{\mathrm{NOON}} \approx \tfrac{1}{4}\, x^4\, \mathrm{csch}^2\left(\tfrac{1}{2}\, x\right)[1 + |g_{\mathrm{M}} - \beta_n(t)|^2\, \sinh(x)]. \tag{21}$$

As shown by Eq. (21), the presence of mechanical loss leads to oscillation in QFI over time. Taking into consideration the first approximation of optical mode loss, the energy variance calculation for the system yields an expression for the QFI as follows:

$$\bar{\mathcal{Q}}^{\kappa,\,\mathrm{SLD}}_{\mathrm{NOON}} \approx \tfrac{1}{4}\, x^4\, \mathrm{csch}^2\left(\tfrac{1}{2}\, x\right)\left[1 + N(t)\, g_{\mathrm{M}}^2\, \sinh\left(\tfrac{1}{2}\, x\right)\right], \tag{22}$$

where $N(t) = (n-2)^2 + 4(n-1)\cos(\omega_{\mathrm{M}} t)$. When $\cos(\omega_{\mathrm{M}} t)$ is maximum, QFI increases correspondingly. However, over time, this value decreases and becomes negative, resulting in significant in the QFI. Consequently, the presence of loss in the optical mode can dramatically reduce the maximum achievable FI. Figure 4 displays the QFI versus temperature ($T$) and the dimensionless time ($\tau = \omega_{\mathrm{M}} t$), considering the initial input field to contain either $n = 2$ (top panels) or $n = 8$ (bottom panels) entangled photons. Also, Fig. 4 shows the impact of dissipation on an input signal consisting of $n = 2$ (top panels) or $n = 8$ (bottom panels) entangled photons. Comparing the size of Fisher's information in the Figure reveals that using a quantum resource, e.g., entanglement, increases quantum information, as expected.

### C. Improved temperature estimation through measured phase analysis

By using optical interferometer devices, it is possible to detect changes in the phase of light as a response to a mechanical movement. They provide a direct measurement of mechanical position by using either a homodyne or heterodyne detector. In a homodyne detector, the signal is interfered with by a local oscillator, while in a heterodyne detector, a

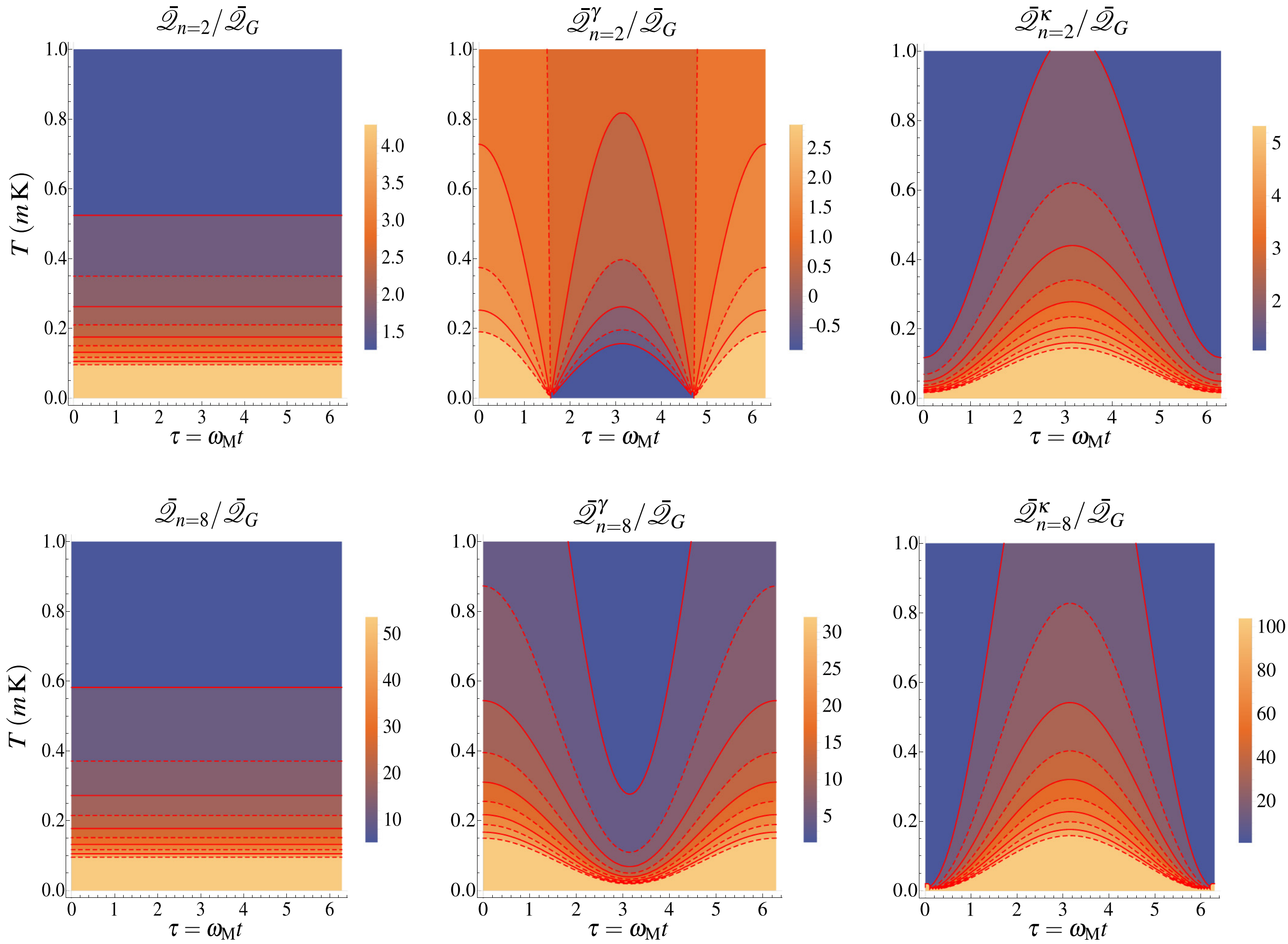

FIG. 4. Contour plots of the ratio of FI changes to Gibbs FI ($\bar{\mathcal{Q}}/\bar{\mathcal{Q}}_G$) in three different scenarios: closed system, open system with mechanical loss, and open system with optical loss. Two input states were used, one with two entangled photons and the other with eight entangled photons. The distinction between the effects of mechanical and optical loss is noticeable in Fisher's function. The size of Fisher's information changes dramatically as the number of photons increases. Within the temperature range, the loss effect leads to the contraction and displacement of the maximum amount of FI. During this period, the changes occur alongside a revival and decline process. This diagram was created using experimental data from the optomechanical cavity that meets the condition $g_0 \gg \omega_{\mathrm{M}}$. The relevant parameter values are $g_{\mathrm{M}} = 14.29$, $\gamma_{\mathrm{M}} = 0.024$, and $\kappa_{\mathrm{M}} = 16$ [49].

local oscillator of a different frequency is mixed with the signal [58–61]. Therefore, the phase measurement is a fundamental tools to determine physical properties of systems. Furthermore, to measure small phase differences, the use of entangled states can lead to major improvements in measurement outcomes of an interferometer. However, the quantum mechanics places a fundamental limit on our ability to make measurements, and the phase measurement is a convenient area to investigate this limit. Although there is no Hermitian phase operator with all the desired properties, the Suskind-Glogower operator can play the role of $e^{i\hat{\phi}}$ and can be used to extract the phase. Thus, interferometers with $N$ photons, instead of a single photon, can improve the resolution and sensitivity of the measurement. The parameter of interest $\hat{\phi}^{\{n\}}$ is directly proportional to the phase and visibility that can be obtained through careful measurement. Consequently, the measurement of phase-dependent observables can be utilized to establish the temperature of systems.

The parameter of interest $\hat{\phi}^{\{n\}}$ serves as a quantitative indicator of the photon transition within the device. Its magnitude is directly proportional to the phase and visibility that can be obtained through careful measurement. To determine the values in the $\hat{\rho}_{\mathrm{O}}^{\{n\}}(t)$ state, the Suskind-Galgower phase operator, described by Eq. (11) must be applied. The estimated value $\hat{\phi}^{\{n\}}$ representing the photon transition within the device is directly related to the measured phase and its visibility. Consequently, the measurement of phase-dependent observables can be utilized in temperature estimation. We can now compute the values of $\langle\hat{\phi}^{\{n\}}\rangle$ and $\langle(\hat{\phi}^{\{n\}})^2\rangle$ as follows:

$$\langle\hat{\phi}^{\{n\}}\rangle_{\hat{\rho}_{\mathrm{O}}^{\{n\}}(t)} = e^{-\frac{1}{2}(2n_{\mathrm{th}}+1)n^2\,|\eta(t)|^2}\,\cos[n^2\,\theta_{\mathrm{s}}(t)],$$
$$\langle(\hat{\phi}^{\{n\}})^2\rangle_{\hat{\rho}_{\mathrm{O}}^{\{n\}}(t)} = 1.$$

By conducting several experiments, we can obtain distinct values for the phases that are independent of each other. Then, we can perform statistical analysis to calculate the standard deviation or uncertainty related to the phase measurement, $\Delta\hat{\phi}^{\{n\}}$. Such a methodology enables the attainment of reliable and accurate results. When analyzing a set of measurements, it is crucial to determine the error associated with the data accurately. This can be expressed as $\Delta\hat{\phi}^{\{n\}}_{\text{mean}} = \Delta\hat{\phi}^{\{n\}}/\sqrt{N}$, where $N$ represents the total number of measurements used. This equation underlines the significance of properly assessment the error to ensure scientific findings are reliable and valid. According to the above result and the "average standard error theorem" [62], performing $N$ number of tests that are independent of each other and acted on the same input states leads to the reduction of the uncertainty of the average value of the phase measurement, $(\bar{\phi})$, with the coefficient $\sqrt{N}$. Based on the relationship between temperature and phase, the precision or reliability in estimating temperature can be expressed as

$$\Delta T = |d\langle\hat{\phi}^{\{n\}}\rangle/d\phi|^{-1}\, \Delta\hat{\phi}^{\{n\}}_{\text{mean}}. \tag{23}$$

This formula highlights the importance of accurately estimating phase to achieve precise temperature measurements. The signal-to-noise (SNR) ratio in temperature estimation, denoted as $T/\Delta T$, can be captured by rearranging the previous formula as

$$\text{SNR}^{\{n\}} = \sqrt{N}\, n^2 \left(\frac{g_0}{\omega_{\text{M}}}\right)^2 \sin^2\left(\frac{1}{2}\,\omega_{\text{M}}\, t\right) \text{csch}^2\left(\frac{1}{2}\,x\right)\frac{F_n}{x}, \tag{24}$$

where $F_n = \{e^{n^2\,|\eta(t)|^2\,\coth(\frac{x}{2})}\,\sec^2[n^2\,\theta_{\text{s}}(t)] - 1\}^{-1/2}$.

Upon initial examination, the scaling coefficient $\sqrt{N}\,n^2$ presented in Eq. (24) suggests the possibility of surpassing the Heisenberg limit ($\sqrt{N}\,n$). In light of the preceding discussion, it is worth noting that upon performing an experiment $N$ number of times on an entangled state comprised of $N$ photons, the CRB serves to establish the upper limit of sensitivity that we can attain. Specifically, we can quickly get that this limit is equivalent to $N^{5/2}$. It is worth noting that the parameter denoting the number of photons, represented by the variable $N$, is also a factor in other terms. Due to this consideration, even in instances where $n$ takes on small values, the resulting outcome is found to be of the same magnitude as the Heisenberg limit. The precision value for temperature measurement for three modes with varying numbers of entangled photons and two different values of the $g_{\text{M}}$ are presented in Table I. We set the consecutive time intervals of the measurement to obtain the maximum value of the temperature-dependent exponential function. We should note that the results presented are only for one repetition of the experiment. As indicated in Table I, the degree of precision required falls below $5.7 \times 10^{-7}$, representing the most favorable level of accuracy in temperature assessment [57]. Upon comparison with the data presented in the table, it is evident that the scenario in which $g_0/\omega_{\text{M}} = 14.329$ yields an exact measurement outcome, exhibiting minimal statistical error aside from systematic errors.

TABLE I. Temperature measurement accuracy: The accuracy of temperature measurement for different temperature values is calculated in two optomechanical systems with different coupling coefficients. The right columns of the table show the temperature accuracy, $\Delta T/T$, of two different systems. The first system is linked to its quantum coupling when $g_{\text{M}} = 2.2 \times 10^{-3}$ [56] and the second system for $g_{\text{M}} = 14.29$ [49]. If the value of $g_{\text{M}} \leqslant 1$, then the thermometer system will not be suitable for thermometric. The parameter $n$ represents the number of entangled photons that enter the system. It is worth noting that the minimum acceptable accuracy size according to standards and metrology organization is $5.7 \times 10^{-7}$. Zero values for measurement accuracy indicate a precise measurement.

| $g_{\text{M}}$ | | $2.2 \times 10^{-3}$ | 14.29 |
|---|---|---|---|
| $n$ | $T$ | $\Delta T/T$ $(< 5.7 \times 10^{-7})$ [57] | |
| 1 | 1 μK | 6.15 | $4.4 \times 10^{-181}$ |
| | 1 mK | $5.8 \times 10^{-2}$ | 0.0 |
| | 1 K | $7.41 \times 10^{-14}$ | 0.0 |
| 3 | 1 μK | $2.26 \times 10^{8}$ | 0.0 |
| | 1 mK | $2.11 \times 10^{-3}$ | 0.0 |
| | 1 K | $1.06 \times 10^{-29}$ | 0.0 |
| 5 | 1 μK | $4.89 \times 10^{7}$ | 0.0 |
| | 1 mK | $4.4 \times 10^{-4}$ | 0.0 |
| | 1 K | $6.38 \times 10^{-60}$ | 0.0 |

## IV. CONCLUSION

The present study proposes a different method for precisely measuring temperature through the use of an optomechanical system placed at one of the arms of the Michelson interferometer. By considering the condition $g_0 \gg \omega_{\text{M}}$, which implies that optomechanical coupling is more significant than mechanical frequency, we demonstrate that this system can serve as a highly sensitive thermometer. Notably, prior experimental work has already established this condition for the optomechanical system, as evidenced in Ref. [49]. In this paper, we theoretically investigate this problem in three distinct models: a closed system, an open system with the presence of loss in the mechanical mode, and an open system with loss in its optical mode. Our findings have significant implications for the development of accurate and sensitive temperature measurement technologies, particularly in the fields of physics and engineering.

The experimental setup under consideration constitutes an example of indirect measurement. Our analysis reveals that the presence of a loss in the mechanical mode only has a minimal impact on the overall shape of the Fisher Information (FI). However, optical field loss, resulting from the measurement of the field component, causes a rapid reduction in the range of FI. Specifically, we find that this reduction is quadratic in the zeroth order of the optical loss coefficient.

In addition to that, our study examines the effects of the dissipation of optical and mechanical mode on Fischer information, and also we explore entanglement as a pure quantum resource. Our findings reveal that the presence of entangled photons in the lossless system serves two effects. First, it reduces the time interval required for FI to reach its maximum value, thereby allowing for more measurements to be conducted in the same time frame by the experimenters. Second, the inclusion of entangled photons expands the range of FI, ultimately leading to promoted sensitivity in parameter estimation. The impact of entangled photons on FI is dependent upon the presence or absence of mechanical and optical losses.

Based on our analysis, we can conclude that to enhance the sensitivity of temperature parameter estimation, we should take into account three critical factors in the interferometric setup that the optomechanical system is on one of its arms. First, the optomechanical coupling coefficient's magnitude must be considered significantly greater than the mechanical frequency. Second, the measurement sequence should be adjusted when the Fisher function reaches its maximum value. Finally, to control the loss in the system, one should utilize the entangled photons.

### ACKNOWLEDGMENTS

The authors are grateful to Dr. F. Bemani for providing valuable comments and engaging in fruitful discussions. Finally, we would like to thank the Vice President for Research of the University of Isfahan for its support.

### APPENDIX A: OBTAINING STATE DENSITY MATRIX IN A CLOSED SYSTEM

From Hamiltonian (5) and by using of polaron transformation [63,64], we have

$$\hat{U}_{\rm OM}(t) = e^{-i\,\omega_{\rm R}\,t\,\hat{a}^\dagger\hat{a}} e^{i\,\theta_s(t)(\hat{a}^\dagger\hat{a})^2} e^{\hat{a}^\dagger\hat{a}[\eta(t)\,\hat{b}^\dagger-\eta^*(t)\,\hat{b}]} e^{-i\,\omega_{\rm M}\,t\,\hat{b}^\dagger\hat{b}}. \tag{A1}$$

By applying the unitary transformation operator (A1) on the initial state of the system, Eq. (9), we have

$$\begin{aligned}\hat{\rho}^{\{n\}}_{\rm OM}(t) &= \hat{U}(t)\hat{\rho}^{\{n\}}_{\rm OM}(0)\hat{U}^\dagger(t)\\ &= \tfrac{1}{2}\sum_{j=0}^{\infty}\rho_{j\,j}\big[e^{i\,n^2\,\theta_s(t)}\,|n_{\rm A},\,0_{\rm B};\,j,n\,\eta(t)\rangle\\ &\quad+|0_{\rm A},n_{\rm B};\,j\rangle\big]\\ &\quad\times\,\big[\langle j;\,n_{\rm B},\,0_{\rm A}|+e^{-i\,n^2\,\theta_s(t)}\,\langle n\,\eta(t),\,j;\,0_{\rm B},\,n_{\rm A}|\big].\end{aligned} \tag{A2}$$

Now, with use of $\mathcal{P}(\phi|T)=\mathrm{Tr}\{\hat{\phi}\,\rho_{\rm OM}(\tau)\}$ and Eq. (2), the FI function can be calculated.

### APPENDIX B: EVOLUTION OF OPEN SYSTEM (MECHANICAL MODE): SOLVING THE CHARACTERISTIC FUNCTION

When the mechanical mode is in thermal equilibrium with its environment at temperature $T$, using the optomechanical Hamiltonian (5), the Lindblad equation in the interaction picture is written as follows [65]:

$$\begin{aligned}\dot{\hat{\rho}}_{\rm OM}(\gamma,\,t) &= -[\omega_{\rm M}\hat{a}^\dagger\hat{a}(\varepsilon\hat{b}^\dagger-\varepsilon^*\hat{b}),\;\hat{\rho}_{\rm OM}(\gamma,\,t)]\\ &\quad+\gamma(n_{\rm th}+1)\mathcal{D}_{\hat{b}}[\hat{\rho}_{\rm OM}(\gamma,\,t)]\\ &\quad+\gamma n_{\rm th}\mathcal{D}_{\hat{b}^\dagger}[\hat{\rho}_{\rm OM}(\gamma,\,t)],\end{aligned} \tag{B1}$$

where $\mathcal{D}_{\hat{o}_1\hat{o}_2}[\rho]=\hat{o}_2\rho\hat{o}_1-\frac{1}{2}\{\rho,\;\hat{o}_1\hat{o}_2\}$ and $i\varepsilon=e^{i\omega_{\rm m}t}$. We assume that the system initially prepared in a tensor product of the mechanical mode in the thermal state and the optical mode in number state as follows:

$$\begin{aligned}\rho_{\rm OM}(t=0) &= \rho_{\rm O}(t=0)\otimes\rho_{\rm M}(t=0)\\ &= \sum_{n,m}c_n\,c_m^*\,|n\rangle\langle m|\otimes\sum_{j=0}^{\infty}\frac{n_{\rm th}}{(1+n_{\rm th})^{j+1}}\,|j\rangle\langle j|.\end{aligned} \tag{B2}$$

To determine the time-dependent solution of the above master equation, we follow the procedure similar to that found in Refs. [66–69]. By utilizing the initial state given in Eq. (B2), we can calculate the density matrix of the whole system at time $t$ as

$$\rho_{\rm OM}(t)=\sum_{n,m;j}C_{nm}(t)\,|n\rangle\langle m|\,|j,\alpha_n(t)\rangle\langle\beta_m(t),\,j|, \tag{B3}$$

where the states $|j,\alpha_n(t)\rangle$ represent the displeased number state of the mechanical mode; these states are a broader class of transformed states that can be obtained by applying the displacement operator on arbitrary number states.

Since $\hat{a}^\dagger\hat{a}$ is a constant of motion, we can consider the elements of $C_{nm}(t)$ to be independent of each other. The purpose of calculating the characteristic function is as follows:

$$\chi_{nm}(\lambda,\,t)=\mathrm{Tr}_M\{e^{\lambda\,\hat{b}^\dagger-\lambda^*\,\hat{b}}\,\rho_{nm}(t)\}. \tag{B4}$$

Using the method detailed in Refs. [66–69], the following differential equation for the characteristic function is obtained:

$$\begin{aligned}\hat{\chi}_\gamma(\lambda,\,t) &= e^{i\,\Delta\,t(n-m)}\exp\big\{-\tfrac{1}{2}\gamma t(2n_{\rm th}+1)|\lambda|^2\\ &\quad-\tfrac{1}{2}\,i\,g_0\,t(n+m)(\lambda+\lambda^*)\\ &\quad+[\zeta\,\lambda+i\,g_0(n-m)]\partial_\lambda\\ &\quad-[\zeta^*\,\lambda^*-i\,g_0(n-m)]\partial_{\lambda^*}\big\}\hat{\chi}_\gamma(\lambda,\,0).\end{aligned}$$

Algebraic techniques can be used to solve this equation and determine the value of function $\chi_\gamma(\lambda,\,t)$. Thus, we obtain

$$\begin{aligned}\chi_\gamma(\lambda,\,t) &= e^{i\Delta(n-m)t}\,e^{i\,\theta_t(t)\left(n^2-m^2\right)}\,e^{-(2n_{\rm th}+1)(n-m)^2\theta_\gamma(t)}\\ &\quad\times\left[\tfrac{1}{2}e^{-\frac{1}{2}(2n_{\rm th}+1)|\lambda|^2}\right]\\ &\quad\times e^{\frac{i\,g_0}{2\zeta^*}\left(1-e^{\zeta^*t}\right)(n+m)\lambda^*}\,e^{\frac{i\,g_0}{2\zeta}\left(1-e^{\zeta t}\right)(n+m)\lambda}\\ &\quad\times e^{\frac{-i\,g_0\,\gamma}{2|\zeta|^2}\left(1+\frac{\zeta^*}{\gamma}\right)\left(1-e^{\zeta^* t}\right)(n-m)(2n_{\rm th}+1)\lambda^*}\\ &\quad\times e^{\frac{i\,g_0\,\gamma}{2|\zeta|^2}\left(1+\frac{\zeta}{\gamma}\right)\left(1-e^{\zeta t}\right)(n-m)(2n_{\rm th}+1)\lambda},\end{aligned}$$

where

$$\zeta=i\omega_{\rm M}-\tfrac{1}{2}\gamma,\quad\zeta^*=-i\omega_{\rm M}-\tfrac{1}{2}\gamma.$$

By rearranging the terms according to the characteristic function as

$$\hat{\chi}_\gamma(\lambda,\,t)=\mathrm{Tr}_M\left\{e^{\lambda\hat{b}^\dagger-\lambda^*\hat{b}}\sum_{j=0}^{\infty}\rho_{j\,j}(t)\,|j,\;\beta_n\rangle\langle\beta_m,\;j|\right\},$$

we can obtain

$$\hat{\rho}_{\rm OM}(\kappa,\,t)=\sum_{nm}\sum_{j=0}^{\infty}\rho_{j\,j}(t)\,|n;\;j,\;\beta_n\rangle\langle\beta_m,\;j;\;m|. \tag{B5}$$

## APPENDIX C: EVOLUTION OF OPEN SYSTEM (OPTICAL MODE)

The effect of decoherence on the optical mode can be explained by the Lindblad master equation. We can ignore mechanical attenuation because the radiation mode relaxes much faster than a mechanical mode, so for the Hamiltonian (5) the following quantum master equation is obtained [65]:

$$\dot{\hat{\rho}}_{\rm OM}(\kappa;t) = \frac{1}{i\hbar}[\hat{H}_{\rm OM},\ \hat{\rho}_{\rm OM}(\kappa;t)] + \kappa\,\mathcal{D}_{\hat{a}}[\hat{\rho}_{\rm OM}(\kappa;t)], \quad \text{(C1)}$$

where the number of thermal photons is ignored at optical frequencies, i.e., we assume the zero thermal occupation ($k_{\rm B}\,T/\hbar\,\omega_{\rm R} \approx 0$) for the optical fields; which is a valid approximation at room temperature, despite the fact that for microwave fields it may not be correct [34].

The system without damping has an exact solvable solutions as Eq. (A2) with the free evolution operator $\hat{U}(t)$ where it satisfies the equation $i\,\dot{\hat{U}}(t) = \hat{H}\,\hat{U}(t)$. By using the unitary time evolution operator used in the closed system (A1), we modify the master quantum equation (C1) to obtain an integral equation [63]. By performing the time derivative, using the equation related to time changes $\hat{U}$ and noting that at $t = 0$ the initial state is independent of time, the following relationship can be concluded:

$$\partial_t[\hat{U}_t^\dagger\,\hat{\rho}_{\rm OM}(\kappa;t)\,\hat{U}_t - \hat{\rho}_{\rm OM}(0)] = \kappa\,\hat{U}_t^\dagger\,\mathcal{D}_{\hat{a}}[\hat{\rho}_{\rm OM}(\kappa;t)]\,\hat{U}_t.$$

By using the unitary property of the time evolution operator, Eq. (C1) becomes a first-order differential equation with the following solution:

$$\hat{\rho}_{\rm OM}(\kappa;t) = \hat{\rho}_{\rm OM}(t) + \hat{\rho}_{\mathcal{D}}(t), \quad \text{(C2)}$$

where

$$\hat{\rho}_{\mathcal{D}}(t) = \kappa\,\hat{U}_t\left\{\int_0^t dt'\,\hat{U}_{t'}^\dagger\mathcal{D}_{\hat{a}}\big[\hat{\rho}_{\rm OM}(\kappa;t')\big]\,\hat{U}_{t'}\right\}\hat{U}_t^\dagger. \quad \text{(C3)}$$

The equation of linear integrals of this kind can be solved by successive approximations in which we can consider the initial nearness guess for our unknown density operator as [70]

$$\hat{\rho}_{\rm OM}(\kappa;t') \approx \hat{\rho}_{\rm OM}^{\{n\}}(t'). \quad \text{(C4)}$$

A necessary and sufficient condition for the correctness of the above approximations is that the integral terms in Eq. (C3) are much smaller than the density operator $\hat{\rho}_{\mathcal{D}}(t) \ll \hat{\rho}_{\rm OM}(t)$. It can also be easily verified that ${\rm Tr}_{\rm OM}\{\hat{\rho}_{\mathcal{D}}(t)\} = 0$, therefore, the density operator $\hat{\rho}_{\rm OM}(\kappa;t)$ is always normalized to unity. So we can solve the integral equation in Eq. (C2) using the approximate solution (A2) and obtain

$$\begin{aligned}
&\hat{\rho}_{\rm OM}^{\{n\}}(\kappa,\ t)\\
&\approx \tfrac{1}{2}\sum_{j=0}^{\infty}\rho_{j\,j}\,[|0_{\rm A}\,n_{\rm B};\ j\rangle\langle j;\ n_{\rm B}\,0_{\rm A}|\\
&\quad + (1 - n\,\kappa\,t)|n_{\rm A}\,0_{\rm B};\ j,\ n\eta(t)\rangle\langle n\eta(t),\ j;\ 0_{\rm B}\,n_{\rm A}|\\
&\quad + \left(1 - \tfrac{1}{2}\,n\,\kappa\,t\right)|n_{\rm A}\,0_{\rm B};\ j,\ n\eta(t)\rangle\langle j;\ n_{\rm B}\,0_{\rm A}|\,e^{i\,n^2\,\theta_s(t)}\\
&\quad + \left(1 - \tfrac{1}{2}\,n\,\kappa\,t\right)|0_{\rm A}\,n_{\rm B};\ j\rangle\langle n\eta(t),\ j;\ 0_{\rm B}\,n_{\rm A}|\,e^{-i\,n^2\,\theta_s(t)}\\
&\quad + \kappa\int_0^t dt'\,\big|(n-1)_{\rm A}\,0_{\rm B};\ j,\ (n-1)\eta(t) - \eta^*(t')\\
&\quad \times e^{-i\,\omega_{\rm M}\,t}\big\rangle\\
&\quad \times \big\langle(n-1)\eta(t) - \eta^*(t')\,e^{-i\,\omega_{\rm M}\,t},\ j;\ 0_{\rm B}\,(n-1)_{\rm A}\big|.
\end{aligned} \quad \text{(C5)}$$

## APPENDIX D: CALCULATING QFI USING SLD OPERATOR

The displacement operator property $\hat{D}^{-1}(\alpha)\,\hat{a}\,\hat{D}(\alpha) = \hat{a} + \alpha$ can be employed to perform the calculation of the QFI based on the SLD operator [71]. The Hamiltonian variance in the system state at time $t$ can be calculated by using the following moments:

$$\begin{aligned}
\langle\hat{H}_{\rm OM}\rangle &= {\rm Tr}_{OM}\{\hat{H}_{\rm OM}\,\rho_{\rm OM}(t)\}\\
&= \tfrac{1}{2}\,\{-\hbar\,\Delta + \hbar\,\omega_{\rm M}\langle\eta,\ j|\hat{b}^\dagger\hat{b}|j,\ \eta\rangle\\
&\quad - \hbar\,g_0\langle\eta,\ j|(\hat{b}^\dagger + \hat{b}|j,\ \eta\rangle + \hbar\,\omega_{\rm M}\langle j|\hat{b}^\dagger\hat{b}|j\rangle\}\\
&= \tfrac{1}{2}\,\hbar\,[-\Delta - g_0\,(\eta + \eta^*) + \omega_{\rm M}\,|\eta|^2 + 2\,\omega_{\rm M}\,n_{\rm th}],
\end{aligned}$$

and

$$\begin{aligned}
\big\langle\hat{H}_{\rm OM}^2\big\rangle &= {\rm Tr}_{OM}\big\{\hat{H}_{\rm OM}^2\,\rho_{\rm OM}(t)\big\}\\
&= \tfrac{1}{2}\,\big[\big\langle\eta,\ j|[-\hbar\,\Delta + \hbar\,\omega_{\rm M}\,\hat{b}^\dagger\hat{b} - \hbar\,g_0\big(\hat{b}^\dagger + \hat{b}\big)]^2|j,\ \eta\big\rangle\\
&\quad + \langle j|(\hbar\,\omega_{\rm M}\,\hat{b}^\dagger\hat{b})^2|j\rangle\big].
\end{aligned}$$

So, for the case where $\eta(t) = \frac{g_0}{\omega_{\rm M}}(1 - e^{-i\omega_{\rm M}t})$, the variance is equal to

$$\begin{aligned}
\langle(\Delta\hat{H}_{\rm OM})^2\rangle = \frac{1}{4}\,\beta^{-2}\,x^2\bigg\{&{\rm csch}^2\left(\frac{1}{2}\,x\right)\\
&+ \frac{g_0^2}{\omega_{\rm M}^2}\,{\rm csch}^2\left(\frac{1}{2}\,x\right)\bigg[1 + \sinh\left(\frac{1}{2}\,x\right)\\
&- \cosh\left(\frac{1}{2}\,x\right)\bigg]\bigg\}.
\end{aligned}$$

Therefore, we can calculate $\mathcal{F}_\kappa$ as follows:

$$\mathcal{F}_\kappa = \beta^4\,k_{\rm B}\,\big\langle(\Delta\hat{H}_{\rm OM})^2\big\rangle = \left(\frac{k_{\rm B}}{\hbar\,\omega_{\rm M}}\right)^2\beta^2\,x^2\,\big\langle(\Delta\hat{H}_{\rm OM})^2\big\rangle.$$

## APPENDIX E: ENERGY VARIANCE IN AN ISOLATED OPTOMECHANICAL SYSTEM

Since the variance is a bounded quantity, we can calculate the maximum of energy variance and use it to extract optomechanical energy, determine optimal measurement conditions, and establish the arrangement of energy levels in the system. As the Hamiltonian of the optomechanical system, Eq. (5), commutes with the photon number operator, the number of photons remains constant. Therefore, the energy states of the cavity and the mirror are given by

$$|\epsilon_l\rangle = |n\rangle_{\rm O}|n\,g_0/\omega_{\rm M},\ j\rangle_{\rm M}, \quad n, j = 0, 1, 2, \ldots. \quad \text{(E1)}$$

The Hamiltonian in the subspace of $n$ photons is a harmonic oscillator with frequency $\omega_M$ shifted by $-nx_0$, where $x_0 = -2x_{\rm ZPF}g_0/\omega_M$ is the displacement due to one photon. As a result, the eigenvalues of the optomechanical Hamiltonian with nonnegative integers $n$ and $j$ are given by

$$E_{nj} = E_n + E_j = \hbar\left(\omega_R n - g_0^2 n^2/\omega_M\right) + \hbar\,\omega_M\, j. \tag{E2}$$

The likelihood of selecting one quantum particle from the optomechanical system, with energy $E_{nj}$, is governed by the Boltzmann coefficient $e^{-\beta E_{nj}}$ [72]. In the specific basis of energy states, we represent the density matrix of a cavity containing $N$ photons as

$$\rho_{Nj} = \mathcal{Z}^{-1} e^{-\beta E_N} e^{-\beta E_j}, \quad j = 0, 1, 2, \ldots. \tag{E3}$$

The partition function $\mathcal{Z}$ is determined by its normalization condition. The trace of the density matrix is time independent and must adhere to the relation $\mathrm{Tr}\{\hat{\rho}\} = 1$, thus

$$\mathcal{Z} = e^{-\beta E_N} \sum_{j=0}^{\infty} e^{-\beta E_j}. \tag{E4}$$

Finally, the density matrix of this group of particles is obtained as follows:

$$\hat{\rho} = \sum_{j=0}^{\infty} |N;\, j, Ng_0/\omega_M\rangle\langle Ng_0/\omega_M, j;\, N| \,\frac{e^{-\beta \hat{H}_{\mathrm{OM}}}}{\mathcal{Z}}. \tag{E5}$$

The quantum Gibbs state of the optomechanical system is given by Eq. (E5), which implies that the system is in thermal equilibrium at temperature $T$ and follows the dynamics governed by the Hamiltonian $H$. This definition of Gibbs's state indicates that the system is in a probability distribution at equilibrium that remains constant during its future evolution. To determine the Fisher information, we must calculate the energy variance for this Gibbs state related to the optomechanical system according to the Eq. (4). The variance of the energy in this case is independent of the number of photons inside the cavity and results the Fisher function as follows:

$$\bar{\mathcal{F}}_G = \tfrac{1}{4}\, x^4 \mathrm{csch}^2\left(\tfrac{1}{2}\, x\right). \tag{E6}$$

However, the quantile variance is bounded and therefore its maximum value is determined by examining its derivative with respect to energy

$$\partial_{E_N} \Delta \hat{H}_{\mathrm{O}}^2 = 0. \tag{E7}$$

Hence, the best optomechanical energy can be derived from the subsequent relation [43]

$$(E_{nj} - E_{mk})[E_{nj} + E_{mk} - 2(\langle \hat{H}\rangle + k_B T)] = 0. \tag{E8}$$

The number of photons in the Hamiltonian (5) is a constant value, meaning that either $j$ and $k$ are equal or the following relationship holds:

$$\hbar\,\omega_M(j + k) = 2(\langle \hat{H}\rangle + k_B T - \hbar\,\omega_M N\,\epsilon_N), \tag{E9}$$

where $\epsilon_N = (\omega_R/\omega_M) - (g_0^2/\omega_M^2)N$. This means that the optomechanical system has caused the mechanical oscillator to behave as a two-level system. Thus, if we adjust the spectrum to set $j = 0$, the upper level quantum number is determined by the gap relationship between two energy levels as follows:

$$k = \coth\left(\tfrac{1}{2}\, x\right) + 2/x - 1. \tag{E10}$$


[1] S. Vinjanampathy and J. Anders, Contemp. Phys. **57**, 545 (2016).
[2] R. Alicki and R. Kosloff, Introduction to quantum thermodynamics: History and prospects, in *Thermodynamics in the Quantum Regime: Fundamental Aspects and New Directions*, edited by F. Binder, L. A. Correa, C. Gogolin, J. Anders, and G. Adesso (Springer International Publishing, Cham, Switzerland, 2018), pp. 1–33.
[3] S. Deffner and S. Campbell, arXiv:1907.01596.
[4] J. Monsel, *Quantum Thermodynamics and Optomechanics* (Springer International Publishing, New York, 2020).
[5] G. Kurizki and A. G. Kofman, *Thermodynamics and Control of Open Quantum Systems* (Cambridge University Press, Cambridge, England, 2021).
[6] S. Seah, S. Nimmrichter, D. Grimmer, J. P. Santos, V. Scarani, and G. T. Landi, Phys. Rev. Lett. **123**, 180602 (2019).
[7] M. Mehboudi, A. Sanpera, and L. A. Correa, J. Phys. A: Math. Theor. **52**, 303001 (2019).
[8] E. B. Norrgard, S. P. Eckel, C. L. Holloway, and E. L. Shirley, New J. Phys. **23**, 033037 (2021).
[9] J. Rubio, J. Anders, and L. A. Correa, Phys. Rev. Lett. **127**, 190402 (2021).
[10] J. Boeyens, S. Seah, and S. Nimmrichter, Phys. Rev. A **104**, 052214 (2021).
[11] M. Fujiwara and Y. Shikano, Nanotechnology **32**, 482002 (2021).
[12] M. R. Jørgensen, J. Kołodyński, M. Mehboudi, M. Perarnau-Llobet, and J. B. Brask, Phys. Rev. A **105**, 042601 (2022).
[13] N. Zhang, C. Chen, S.-Y. Bai, W. Wu, and J.-H. An, Phys. Rev. Appl. **17**, 034073 (2022).
[14] J. Fischer, Metrologia **52**, S364 (2015).
[15] M. Hayashi, *Quantum Information: An Introduction*, 1st ed. (Springer Berlin, Heidelberg, 2006).
[16] H. M. Wiseman and G. J. Milburn, *Quantum Measurement and Control* (Cambridge University Press, Cambridge, 2009).
[17] A. Holevo, *Probabilistic and Statistical Aspects of Quantum Theory* (Springer, New York, 2011).
[18] S. L. Braunstein and C. M. Caves, Phys. Rev. Lett. **72**, 3439 (1994).
[19] S. L. Braunstein, C. M. Caves, and G. Milburn, Ann. Phys. (NY) **247**, 135 (1996).
[20] V. Giovannetti, S. Lloyd, and L. Maccone, Nat. Photonics **5**, 222 (2011).
[21] B. C. Sanders and G. J. Milburn, Phys. Rev. Lett. **75**, 2944 (1995).
[22] P. Kok, H. Lee, and J. P. Dowling, Phys. Rev. A **65**, 052104 (2002).
[23] P. Cappellaro, J. Emerson, N. Boulant, C. Ramanathan, S. Lloyd, and D. G. Cory, Phys. Rev. Lett. **94**, 020502 (2005).
[24] S. Boixo, S. T. Flammia, C. M. Caves, and J. M. Geremia, Phys. Rev. Lett. **98**, 090401 (2007).
[25] S. M. Roy and S. L. Braunstein, Phys. Rev. Lett. **100**, 220501 (2008).

[26] T. M. Stace, Phys. Rev. A **82**, 011611(R) (2010).
[27] A. Rivas and A. Luis, Phys. Rev. Lett. **105**, 010403 (2010).
[28] M. Zwierz, C. A. Pérez-Delgado, and P. Kok, Phys. Rev. Lett. **105**, 180402 (2010).
[29] M. Napolitano, M. Koschorreck, B. Dubost, N. Behbood, R. J. Sewell, and M. W. Mitchell, Nature (London) **471**, 486 (2011).
[30] J. Zhang, M. Um, D. Lv, J.-N. Zhang, L.-M. Duan, and K. Kim, Phys. Rev. Lett. **121**, 160502 (2018).
[31] J. Chen and L. F. Wei, Phys. Rev. A **95**, 033838 (2017).
[32] A. Candeloro, S. Razavian, M. Piccolini, B. Teklu, S. Olivares, and M. G. A. Paris, Entropy **23**, 1353 (2021).
[33] M. Asjad, B. Teklu, and M. G. A. Paris, Phys. Rev. Res. **5**, 013185 (2023).
[34] M. Aspelmeyer, T. J. Kippenberg, and F. Marquardt, Rev. Mod. Phys. **86**, 1391 (2014).
[35] M. Jarzyna and M. Zwierz, Phys. Rev. A **92**, 032112 (2015).
[36] G. Adesso, T. R. Bromley, and M. Cianciaruso, J. Phys. A: Math. Theor. **49**, 473001 (2016).
[37] A. Streltsov, G. Adesso, and M. B. Plenio, Rev. Mod. Phys. **89**, 041003 (2017).
[38] E. Chitambar and G. Gour, Rev. Mod. Phys. **91**, 025001 (2019).
[39] S. Barzanjeh, A. Xuereb, S. Gröblacher, M. Paternostro, C. A. Regal, and E. M. Weig, Nat. Phys. **18**, 15 (2022).
[40] C. L. Degen, F. Reinhard, and P. Cappellaro, Rev. Mod. Phys. **89**, 035002 (2017).
[41] K. Jacobs, *Quantum Measurement Theory and its Applications* (Cambridge University Press, Cambridge, England, 2014), pp. 1–544.
[42] V. Giovannetti, S. Lloyd, and L. Maccone, Phys. Rev. Lett. **96**, 010401 (2006).
[43] L. A. Correa, M. Mehboudi, G. Adesso, and A. Sanpera, Phys. Rev. Lett. **114**, 220405 (2015).
[44] W. Marshall, C. Simon, R. Penrose, and D. Bouwmeester, Phys. Rev. Lett. **91**, 130401 (2003).
[45] K. Hammerer, C. Genes, D. Vitali, P. Tombesi, G. Milburn, C. Simon, and D. Bouwmeester, in *Cavity Optomechanics: Nano- and Micromechanical Resonators Interacting with Light* (Springer, Berlin, 2014), pp. 25–56.
[46] A. Nunnenkamp, K. Børkje, and S. M. Girvin, Phys. Rev. Lett. **107**, 063602 (2011).
[47] M. Aspelmeyer, T. J. Kippenberg, and F. Marquardt, *Cavity Optomechanics: Nano- and Micromechanical Resonators Interacting with Light*, Vol. 22 (Springer, Berlin, 2014), pp. 1–357.
[48] W. P. Bowen, *Quantum Optomechanics* (CRC Press, Boca Raton, FL, 2015).
[49] K. W. Murch, K. L. Moore, S. Gupta, and D. M. Stamper-Kurn, Nat. Phys. **4**, 561 (2008).
[50] L. Susskind and J. Glogower, Phys. Phys. Fiz. **1**, 49 (1964).
[51] A. N. Boto, P. Kok, D. S. Abrams, S. L. Braunstein, C. P. Williams, and J. P. Dowling, Phys. Rev. Lett. **85**, 2733 (2000).
[52] D. S. Simon, G. Jaeger, and A. V. Sergienko, Quantum metrology, in *Quantum Metrology, Imaging, and Communication* (Springer International Publishing, Cham, Switzerland, 2017), pp. 91–112.
[53] V. Montenegro, M. G. Genoni, A. Bayat, and M. G. A. Paris, Phys. Rev. Res. **2**, 043338 (2020).
[54] S. Bose, K. Jacobs, and P. L. Knight, Phys. Rev. A **59**, 3204 (1999).
[55] J.-Q. Liao, H. K. Cheung, and C. K. Law, Phys. Rev. A **85**, 025803 (2012).
[56] B. Pepper, D. Bouwmeester, D. Kleckner, E. Jeffrey, P. Sonin, and S. M. Thon, Opt. Exp. **19**, 19708 (2011).
[57] P. J. Mohr, D. B. Newell, and B. N. Taylor, J. Phys. Chem. Ref. Data **45**, 043102 (2016).
[58] G. Huang, A. Beccari, N. J. Engelsen, and T. J. Kippenberg, Nature (London) **626**, 512 (2024).
[59] J. Clarke, P. Neveu, K. E. Khosla, E. Verhagen, and M. R. Vanner, Phys. Rev. Lett. **131**, 053601 (2023).
[60] F. Armata, L. Latmiral, A. D. K. Plato, and M. S. Kim, Phys. Rev. A **96**, 043824 (2017).
[61] A. Buonanno, Y. Chen, and N. Mavalvala, Phys. Rev. D **67**, 122005 (2003).
[62] C. W. Helstrom, *Quantum Detection and Estimation Theory*, Mathematics in Science and Engineering, Vol. 123 (Elsevier, Amsterdam, 1976), p. 309.
[63] S. Mancini, V. I. Man'ko, and P. Tombesi, Phys. Rev. A **55**, 3042 (1997).
[64] S. Bose, K. Jacobs, and P. L. Knight, Phys. Rev. A **56**, 4175 (1997).
[65] H. P. Breuer, E. M. Laine, J. Piilo, and B. Vacchini, Rev. Mod. Phys. **88**, 021002 (2016).
[66] J. Wei and E. Norman, J. Math. Phys. **4**, 575 (1963).
[67] D. F. Walls, M. J. Collet, and G. J. Milburn, Phys. Rev. D **32**, 3208 (1985).
[68] H.-P. Breuer and F. Petruccione, *The Theory of Open Quantum Systems* (Oxford University Press, New York, 2002), pp. 1–656.
[69] D. Walls and G. J. Milburn, in *Quantum Optics*, edited by D. Walls and G. J. Milburn (Springer, Berlin, 2008).
[70] G. B. Arfken, H. J. Weber, and F. E. Harris, in *Mathematical Methods for Physicists (Seventh Edition)*, edited by G. B. Arfken, H. J. Weber, and F. E. Harris (Academic, Boston, 2013), pp. 1047–1079.
[71] M. O. Scully and M. S. Zubairy, *Quantum Optics* (Cambridge University Press, Cambridge, England, 1997).
[72] R. Pathria and P. D. Beale, in *Statistical Mechanics (Fourth Edition)* (Academic, New York, 2022), pp. 361–416.